# Stability of stationary equilibrium solutions of a diffuse interface electrical breakdown model

A. S. Ponomarev[1], E. V. Zipunova[1], E. B. Savenkov[1]
[1]Keldysh Institute of Applied Mathematics, Moscow, Russia

The aim of the present work is to study qualitative characteristics and to perform a numerical analysis of a diffuse interface model describing the development of an electrical breakdown channel in a solid dielectric. Stability of the system equilibrium positions is analysed. Conditions for the breakdown channel development from small perturbations of the intact medium are found. A differential scheme for the problem is constructed and investigated, an informative estimate of its stability is given. The obtained theoretical results are validated by a computer simulation.

Key words and phrases: diffuse interface model, phase field, stability, electrical breakdown.

## 1. Introduction

Electrical breakdown of a solid dielectric is a rapid process, which involves a variety of mutually interrelated physical mechanisms [1]. At present, it is practically impossible to identify and characterize them at the level acceptable for predictive first-principal modelling and simulation. Therefore, a promising approach to the electrical breakdown modelling is to utalize reasonably complex phenomenological models suitable for practical settings analysis.

Among the variety of approaches suggested to describe electrical breakdown, a particular place is occupied by the phase field (or diffuse interface) model originally introduced in [2]. According to the phase field modelling framework, the essentially one dimensional breakdown channel is described using a scalar phase field, i.e., a smooth function $\phi = \phi(\mathbf{x}, t)$ with values within the $[0,1]$ interval. It is assumed that the channel occupies a spatial domain where $\phi = 0$, while in completely undamaged medium $\phi = 1$. The spatial domain with $0 < \phi < 1$ separating damaged and undamaged medium is considered to be a "diffuse" boundary of finite width. The process of the breakdown channel development ("growth") is described as evolution of $\phi$ over time $t$, governed by a physically motivated evolutionary PDE. The damaged and undamaged states of the medium are treated as two different phases. The process itself is described as phase transition between them. The transition occurs under specified conditions. Diffuse interface models are mainly phenomenological ones. In other words, they are mostly based on certain macroscopic laws and fundamental assumptions and do not rely on first-principal physics and elementary mechanisms related to the particular macroscopic problem under consideration.

Today diffuse interface models provide a solid and widely used framework to describe multi-phase phenomena in hydrodynamics [3–5], solid and fracture mechanics [6], material science [7], solidification and phase transition problems [8–10], phase field crystals [11–13].

The model suggested in [2] can be considered as a generalization of widely known diffuse interface models in solid mechanics. The model is investigated and further generalized in [14, 15].

The main aim of this paper is to analyse stability of stationary equilibrium solutions of the

phase-field model for the electrical breakdown development. In fact, it is shown that the development of the electrical breakdown channel in the considered model is closely related to the stability loss of the equilibrium solutions.

The model is considered in its simplest form, as it is presented in [2]. Moreover, a spatially one-dimensional setting is used to perform theoretical analysis. As a final result, a stability condition is formulated in terms of the model parameters. Whenever the condition is violated, the intact medium loses stability and small perturbations cause it to evolve into a breakdown-channel-like structure.

To confirm the obtained theoretical results, we present a simple explicit finite-difference scheme allowing to analyse the breakdown process numerically. Since the goal of our computations is to analyse the instability development of in the initial phase field distribution, a careful and comprehensive analysis of stability for the scheme is performed. The analysis is essential to clearly distinguish between numerical artifacts and the development of "physical" instabilities in the solution. The performed simulation completely confirms the obtained theoretical results.

The structure of the paper is as follows. In section 2 we present the mathematical model considered in the rest of the paper. Section 3 is devoted to the stability analysis of equilibrium solutions. In section 4 we analyse the finite-difference scheme. Finally, in section 5 we present numerical results confirming the theoretical findings. In conclusion, we outline and summarize the main results of the paper.

This work was supported by the Russian Science Foundation, project no. 22-11-00203.

# 2. The mathematical model and problem statement

## 2.1 The mathematical model

Let us discuss briefly the phase-field mathematical model describing the electrical breakdown channel propagation, according to [2]. The model assumes that the electrical breakdown evolution is described as phase transition from the initial, undamaged, state of the medium to its damaged state. The spatial domain occupied by the damaged phase is considered as the breakdown channel. The breakdown channel development is described as a process of formation of the domains occupied by the damaged phase.

We assume that the medium occupies a bounded spatial domain $\Omega \subset \mathbb{R}^3$. The state of the medium is given by two scalar-valued fields: $\phi = \phi(\mathbf{x}, t)$, $\phi : \Omega \times [0, +\infty)_t \to [0,1]$ — the phase field and $\Phi : \Omega \times [0, +\infty)_t \to \mathbb{R}$ — the electric potential.

It is assumed that $\phi$ is continuous and sufficiently smooth with values $\phi \in [0,1]$. The value $\phi = 1$ corresponds to the initial, undamaged, state of the medium, and the value $\phi = 0$ — to the damaged phase, which is related to the state of the medium in the breakdown channel.

The only property of the medium is its electric permittivity $\varepsilon$. Its value depends on the state of the medium and is given by:

$$\varepsilon(\mathbf{x}, t) = \varepsilon[\phi] = \frac{\varepsilon_0(\mathbf{x})}{f(\phi(\mathbf{x}, t)) + \delta}, \quad f(\phi) = 4\phi^3 - 3\phi^4. \tag{1}$$

Here $\varepsilon_0(\mathbf{x})$ is the permittivity of the undamaged medium; $f(\phi)$ is the so-called interpolation

function, smoothly connecting the 0 and 1 values. It is assumed that $f(0)=0$, $f(1)=1$, $f'(0)=f'(1)=0$; $0<\delta\ll 1$ is a small regularizing parameter. Note that at $\phi=1$ we have $\varepsilon(\mathbf{x},t)\approx\varepsilon_0(\mathbf{x})$ (which corresponds to the undamaged phase) and at $\phi=0$ we have $\varepsilon(\mathbf{x},t)=\varepsilon_0(\mathbf{x})/\delta$ (which corresponds to the damaged phase, assumed to be an ideal conductor).

The following expression for the Helmholtz free energy $\Pi$ of the system is postulated:

$$\Pi=\int_\Omega \pi d\mathbf{x}, \tag{2}$$

$$\pi=-\frac{1}{2}\varepsilon[\phi](\nabla\Phi,\nabla\Phi)+\Gamma\frac{1-f(\phi)}{l^2}+\frac{\Gamma}{4}(\nabla\phi,\nabla\phi). \tag{3}$$

Here $\Gamma>0$ and $l>0$ are parameters; $\Gamma$ can be interpreted as the energy needed to create a breakdown channel of unit length, while $l$ is the characteristic width of the diffuse interface.

Evolution of the fields $\phi$ and $\Phi$ is governed by the following system of equations:

$$\frac{\delta\Pi}{\delta\Phi}=0;\qquad \frac{1}{m}\frac{\partial\phi}{\partial t}=-\frac{\delta\Pi}{\delta\phi}. \tag{4}$$

Here $m>0$ is the so-called mobility. It has the meaning of the change speed of $\phi$ under a unit "force" applied. According to (4), the fields evolve in a way to minimize (2).

The explicit form of (4) with $\Pi$ given by (2) is:

$$\operatorname{div}(\varepsilon[\phi]\nabla\Phi)=0; \tag{5}$$

$$\frac{1}{m}\frac{\partial\phi}{\partial t}=\frac{1}{2}\varepsilon'(\phi)(\nabla\Phi,\nabla\Phi)+\frac{\Gamma}{l^2}f'(\phi)+\frac{1}{2}\Gamma\Delta\phi, \tag{6}$$

where $(\cdot)'\equiv(\cdot)'_\phi$ and $(\mathbf{a},\mathbf{b})$ is the dot product. The first equation, (5), in this system is linear in $\Phi$. The second one, (6), is a nonlinear Allen–Cahn type equation.

## 2.2. The one-dimensional problem

Consider a one-dimensional form of (5) and (6). Let the closed domain $\bar{\Omega}$ be $\bar{\Omega}=[0,W]_x\times[0,H]_y\times I_z$, with $W,H>0$ and $I$ being a closed interval. Let $\varepsilon_0(\mathbf{x})=\varepsilon_0(x)$ and also $\phi(\mathbf{x},0)=\phi_0(x)$, — i.e., the distribution of electric permittivity and the initial condition for $\phi$ depend only on the $x$-coordinate. We also assume that the following boundary conditions are defined at $\partial\Omega$: $\phi|_{x=0}=\phi_l(t)$, $\phi|_{x=W}=\phi_r(t)$ and also $\partial\phi/\partial\mathbf{n}=0$ at the faces of $\bar{\Omega}$ perpendicular to the $Oy$ and $Oz$ axes. For $\Phi$ we set: $\Phi|_{y=0}=\Phi^-$, $\Phi|_{y=H}=\Phi^+$, where $\Phi^-,\Phi^+\in\mathbb{R}$, and also $\partial\Phi/\partial\mathbf{n}=0$ at the faces of $\bar{\Omega}$ perpendicular to the $Ox$ and $Oz$ axes. Here $\partial/\partial\mathbf{n}$ denotes the directional derivative along the outward unit normal $\mathbf{n}$ to $\partial\Omega$.

Taking the formulated assumptions into account, the solution of (5),(6) has the form $\phi(\mathbf{x},t)=\phi(x,t)$, $\Phi(\mathbf{x},t)=\Phi(y,t)$, — i.e., $\phi$ does not depend on $y$ and $z$, $\Phi$ — on $x$ and $z$.

Therefore, (5) can be reduced to:

$$0=\operatorname{div}(\varepsilon[\phi]\nabla\Phi)=(\nabla\varepsilon,\nabla\Phi)+\varepsilon\Delta\Phi\equiv\varepsilon\Delta\Phi, \tag{7}$$

since $(\nabla\varepsilon,\nabla\Phi)=0$ as $\varepsilon$ does not depend on $y$ and $z$. The solution of (7) satisfying the boundary conditions is $\Phi(\mathbf{x},t)=\Phi^{-}+(y/H)(\Phi^{+}-\Phi^{-})$.

Substituting the obtained solution for $\Phi$ into (6) we have:

$$\frac{1}{m}\frac{\partial\phi}{\partial t}=\frac{1}{2}\varepsilon'(\phi)\left(\frac{\Phi^{+}-\Phi^{-}}{H}\right)^{2}+\frac{\Gamma}{l^{2}}f'(\phi)+\frac{1}{2}\Gamma\frac{\partial^{2}\phi}{\partial x^{2}}. \tag{8}$$

The solution $\phi(x,t)$ of (8) is defined in the spatially one-dimensional domain $[0,W]_{x}\times[0,+\infty)_{t}$. For further convenience we write (8) as:

$$\frac{1}{m}\frac{\partial\phi}{\partial t}=\frac{1}{2}K_{\Phi}^{2}\varepsilon'(\phi)+\frac{\Gamma}{l^{2}}f'(\phi)+\frac{1}{2}\Gamma\frac{\partial^{2}\phi}{\partial x^{2}},\quad K_{\Phi}=\|\nabla\Phi\|=(\Phi^{+}-\Phi^{-})/H. \tag{9}$$

Note that now the parameters $\Phi^{+}$, $\Phi^{-}$ and $H$ do not enter the considered equation explicitly.

Equation (9) is supplemented by the initial condition

$$\phi(x,0)=\phi_{0}(x) \tag{10}$$

and also by the boundary conditions

$$\phi(0,t)=\phi_{l}(t),\quad \phi(W,t)=\phi_{r}(t). \tag{11}$$

For simplicity of further analysis we also assume that $\varepsilon_{0}(x)=\text{const}$.

So, the pair of functions $\phi$ and $\Phi$, where $\phi$ is the solution of problem (9), (10), (11) and $\Phi$ is given by $\Phi=\Phi^{-}+(y/H)(\Phi^{+}-\Phi^{-})$, satisfies (5), (6) under the provided assumptions.

## 3. Stability analysis of equilibrium solutions

Under certain conditions, the electrical breakdown can develop form small perturbations of the undamaged medium properties. To clarify these conditions, in this section we study stability of constant solutions $\phi(x,t)\equiv C$, $C\in[0,1]$, of equation (9).

First, one has to find stationary constant solutions of (9). From definition (1) follow the expressions for the derivatives of $\varepsilon(\phi)$:

$$\varepsilon'(\phi)=\frac{-\varepsilon_{0}f'(\phi)}{\left(f(\phi)+\delta\right)^{2}};\qquad \varepsilon''(\phi)=\varepsilon_{0}\frac{2(f'(\phi))^{2}-f''(\phi)\left(f(\phi)+\delta\right)}{\left(f(\phi)+\delta\right)^{3}}. \tag{12}$$

Substituting $\phi(x,t)\equiv C$ into (9) and taking (12) into account, one has:

$$f'(C)\left(\frac{\Gamma}{l^{2}}-\frac{1}{2}K_{\Phi}^{2}\frac{\varepsilon_{0}}{\left(f(C)+\delta\right)^{2}}\right)=0. \tag{13}$$

First, consider the case $f'(C)=12C^{2}(1-C)=0$, which leads to $C=0,1$. Hence, $\phi\equiv 0$ and $\phi\equiv 1$ are equilibrium solutions.

Second, let $C\neq 0,1$. Then

$$\frac{\Gamma}{l^2}=\frac{K_\Phi^2\varepsilon_0}{2\left(f\left(C\right)+\delta\right)^2}\quad\text{and}\quad f\left(C\right)+\delta=K_\Phi l\sqrt{\frac{\varepsilon_0}{2\Gamma}}.$$

Note that $f\left(C\right)\in\left[0,1\right]$ and, moreover, $f\left(\phi\right)$ is monotonically increasing. Therefore, in case $K_\Phi l\sqrt{\varepsilon_0/\left(2\Gamma\right)}\in\left(\delta,1+\delta\right)$ equation (13) has a solution $C_3\neq 0,1$ given by

$$C_3=f^{-1}\left(K_\Phi l\sqrt{\frac{\varepsilon_0}{2\Gamma}}-\delta\right). \tag{14}$$

Otherwise equation (13) has only two solutions.

So, the number of constant equilibrium solutions depends on the following condition being satisfied:

$$\delta^2<\frac{K_\Phi^2 l^2\varepsilon_0}{2\Gamma}<(1+\delta)^2. \tag{15}$$

It will be shown later how condition (15) is connected with the stability properties of the equilibrium solutions and equation (9) itself.

Let us now proceed to the stability analysis of the equilibrium solutions.

Let $\phi\left(x,t\right)$ be a solution of (9), $\delta\phi\left(x,t\right)$ be its perturbation. Writing down equation (9) for the perturbed solution $\phi+\delta\phi$, after linearizing we obtain the following equation for $\delta\phi$:

$$\frac{1}{m}\frac{\partial\left(\delta\phi\right)}{\partial t}=\left(\frac{1}{2}K_\Phi^2\varepsilon''\left(\phi\right)+\frac{\Gamma}{l^2}f''\left(\phi\right)\right)\delta\phi+\frac{1}{2}\Gamma\frac{\partial^2\left(\delta\phi\right)}{\partial x^2}. \tag{16}$$

For further analysis it is convenient to write (16) as:

$$\frac{\partial\left(\delta\phi\right)}{\partial t}=A\delta\phi+B\frac{\partial^2\left(\delta\phi\right)}{\partial x^2}, \tag{17}$$

where $A$ and $B>0$ are the respective parameters.

Choosing $\delta\phi=e^{\alpha t}\sin\left(\omega x\right)$, one obtains from (17) the following relation for the parameters of the perturbation:

$$\alpha e^{\alpha t}\sin\left(\omega x\right)=Ae^{\alpha t}\sin\left(\omega x\right)-B\omega^2e^{\alpha t}\sin\left(\omega x\right),$$

from where follows:

$$\alpha=A-B\omega^2. \tag{18}$$

Now it is easy to see that, depending on the value of the coefficient

$$A=\frac{1}{2}K_\Phi^2\varepsilon''\left(C\right)+\frac{\Gamma}{l^2}f''\left(C\right),$$

three cases arise:

1. $A>0$. In this case, from $\omega^2\in\left[0,A/B\right)$ it follows that $\alpha>0$, i.e., there exists a perturbation $\delta\phi$ growing in time. Hence, the equilibrium solution $\phi\equiv C$ is unstable.

2. $A<0$. Then, for an arbitrary $\omega$ remains $\alpha\leqslant A<0$. Next, any perturbation $\delta\phi$ in the interval $[0,W]_x$ can be represented as Fourier integral over harmonics decreasing at least as the harmonic for $\omega=0$. Hence, the equilibrium solution $\phi\equiv C$ is stable.

3. $A=0$. Repeating the same reasoning as in the case $A<0$, one can observe that there exist arbitrarily slowly decreasing harmonics (i.e., harmonics with arbitrarily small values of $\alpha$). This case corresponds to neutral stability of the equilibrium solution, and linear analysis does not provide complete information. This case will be considered in more details later.

We now proceed to the discussion of the particular equilibrium states.

Consider the equilibrium solution $\phi\equiv 0$. One has $f''(0)=0$, $\varepsilon''(0)=0$ (see (12)), which leads to $A=0$. As it was noted before, this case requires an elaborate analysis, which will be performed later.

Consider the equilibrium solution $\phi\equiv 1$. In this case $f''(0)=-12$, $\varepsilon''(0)=12\varepsilon_0/(1+\delta)^2$ (see (12)). As a result, we obtain:

$$A=\frac{1}{2}K_\Phi^2\varepsilon''(C)+\frac{\Gamma}{l^2}f''(C)=\frac{6K_\Phi^2\varepsilon_0}{(1+\delta)^2}-\frac{12\Gamma}{l^2}.$$

The equilibrium state is stable if $A<0$, i.e., if

$$\frac{K_\Phi^2 l^2\varepsilon_0}{2\Gamma}<(1+\delta)^2. \tag{19}$$

For this case of an unstable equilibrium, let us find $\omega_0$ such that increasing harmonics are replaced by decreasing ones. To do this, consider (18) with $\alpha=0$, $B=\Gamma/2$ and $A$ given above to obtain:

$$0=\frac{6K_\Phi^2\varepsilon_0}{(1+\delta)^2}-\frac{12\Gamma}{l^2}-\frac{\Gamma}{2}\omega_0^2,$$

from where follows:

$$\omega_0=2\sqrt{\frac{3K_\Phi^2\varepsilon_0}{\Gamma(1+\delta)^2}-\frac{6}{l^2}}.$$

Note that condition (19) is exactly the right-hand side of inequality (15). To explain this and to form a complete picture of what is happening, let us look at the equilibrium solutions from a slightly different perspective.

Solving equation (13), we were finding the zeros of the function

$$\chi(\phi)=\frac{1}{2}K_\Phi^2\varepsilon'(\phi)+\frac{\Gamma}{l^2}f'(\phi). \tag{20}$$

Hence, each equilibrium solution $\phi\equiv C$ uniquely corresponds to a zero $C$ of the function $\chi(\phi)$. From the derivation of equation (16) for the perturbation it follows that in its right-hand side the coefficient at $\delta\phi$ is $\chi'(\phi)$. Later, analyzing equation (17) for an equilibrium solution $\phi\equiv C$, we considered several cases depending on the sign of the coefficient $A$, which turns out to be exactly $\chi'(C)$.

Summing up the results, one can state the following. The function $\chi(\phi)$ defined by (20) is smooth on $[0,1]$ and always has zeros $C_1=0$ and $C_2=1$. The third zero $C=C_3\in(0,1)$ exists under condition (15). Each equilibrium solution $\phi\equiv C$ uniquely corresponds to a zero of the function $\chi(\phi)$. Their stability properties are described in terms of the sign of $\chi'(\phi)$ at the zeros: positive

values of $\chi'$ correspond to unstable solutions, and negative values — to stable ones.

It is also clear that in the case of vanishing $\chi'$ (as for $\phi = 0$) the linear analysis is not enough — it is necessary to analyse the sign of the first higher-order non-vanishing derivative of $\chi$ — the equilibrium solution is stable if this derivative is negative and unstable if it is positive.

Finally we show that $\chi(\phi)$ has a non-vanishing derivative at its zero $C = C_3 \in (0,1)$ (if the latter exists). Indeed, one has:

$$\chi(C_3) = f'(C_3)\left(\frac{\Gamma}{l^2} - \frac{K_\Phi^2 \varepsilon_0}{2\left(f(C_3)+\delta\right)^2}\right) = 0.$$

Taking into account that $f'(C_3) \neq 0$, one obtains:

$$\frac{\Gamma}{l^2} - \frac{K_\Phi^2 \varepsilon_0}{2\left(f(C_3)+\delta\right)^2} = 0.$$

Then:

$$\chi'(\phi)\Big|_{C_3} = f'(C_3)\left(\frac{\Gamma}{l^2} - \frac{K_\Phi^2 \varepsilon_0}{2\left(f(\phi)+\delta\right)^2}\right)\Bigg|_{C_3} = \left[f(C_3)\right]^2 \frac{K_\Phi^2 \varepsilon_0}{\left(f(C_3)+\delta\right)^3} \neq 0.$$

Now it is possible to provide a comprehensive analysis of the behavior of $\chi(\phi)$ at its zeros. As it can be seen from conditions (15) and (19), its behavior is governed by the value of the parameter

$$\xi = \frac{K_\Phi^2 l^2 \varepsilon_0}{2\Gamma}. \tag{21}$$

First, consider the case $0 \leqslant \xi < \delta^2$. The zeros of $\chi(\phi)$ are 0 and 1; $\chi'(0) = 0$, $\chi'(1) < 0$. The qualitative behavior of $\chi(\phi)$ is shown schematically in Fig. 1. It can be seen that the equilibrium solution $\phi \equiv 0$ is unstable and $\phi \equiv 1$ is stable. Such case can be conventionally called a case of "weak electric field". This means that with all the parameters except the electric field being fixed, the latter is so small that even an almost completely damaged medium with $\phi \approx 0$ is "healed" over time and evolves to the completely undamaged state $\phi \approx 1$.

Second, consider the case $\delta^2 < \xi < (1+\delta)^2$. The zeros of $\chi(\phi)$ are $C = 0$, $C = C_3$ (see (14)) and $C = 1$; $\chi'(0) = 0$, $\chi'(1) < 0$; $\chi'(C_3) > 0$ (since $\chi$ is smooth). The behavior of $\chi(\phi)$ in this case is shown in Fig. 2. The equilibrium solutions are: $\phi \equiv 0$ — a stable one, $\phi \equiv C_3$ — an unstable one, and $\phi \equiv 1$ — also a stable one. Such case can be conventionally called a case of "medium electric field". This means that as the values of $\phi$ are sufficiently close to 0, the damage increases, i.e., $\phi$ tends to zero; as the values of $\phi$ are sufficiently close to 1, the damage decreases, i.e., $\phi$ tends to one; at certain intermediate values the equilibrium is unstable.

Finally, consider the case $(1+\delta)^2 < \xi$. The zeros of $\chi(\phi)$ are $C = 0$ and $C = 1$; $\chi'(0) = 0$, $\chi'(1) > 0$. The qualitative behavior of $\chi(\phi)$ is schematically shown in Fig. 3. The

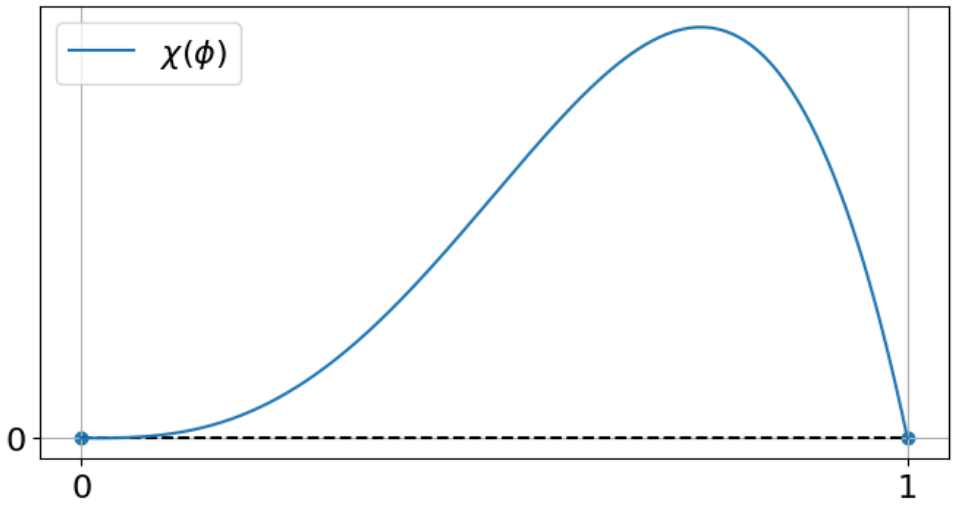


Figure 1. Characteristic behavior of $\chi(\phi)$, a "weak electric field" case.

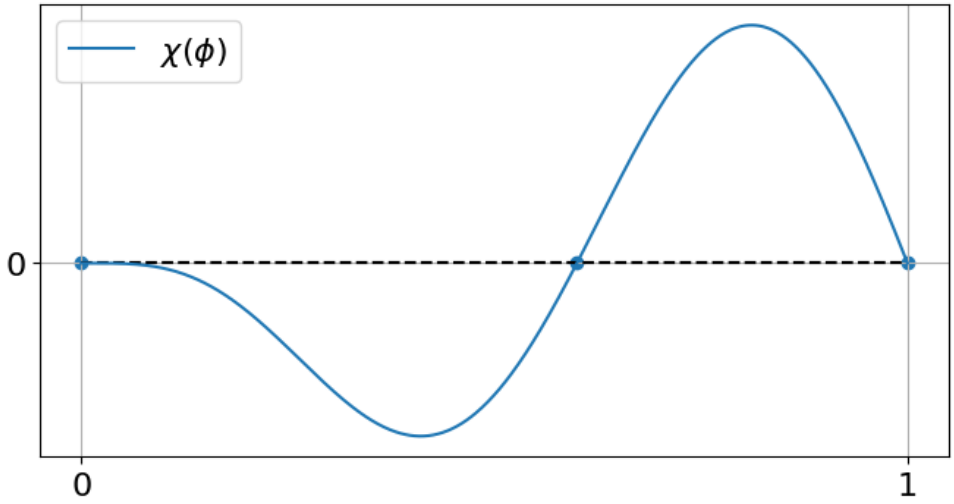


Figure 2. Characteristic behavior of $\chi(\phi)$, a "medium electric field" case.

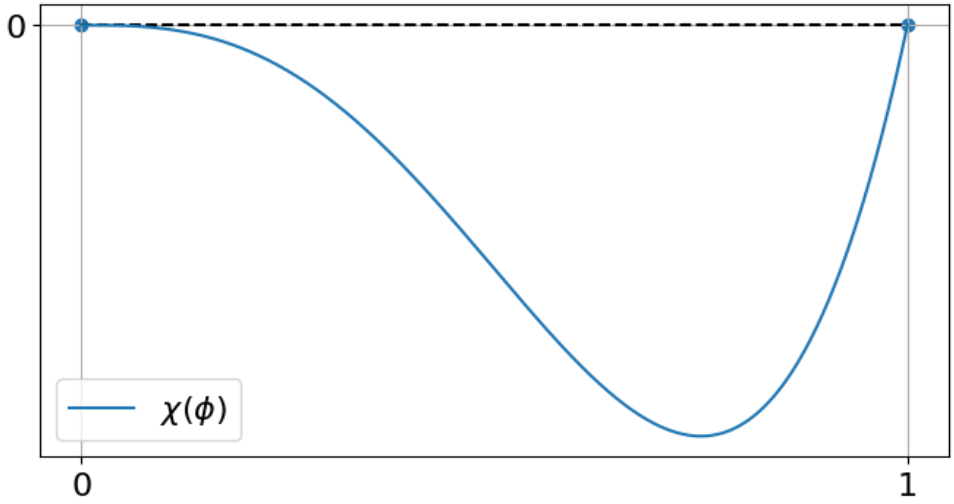


Figure 3. Characteristic behavior of $\chi(\phi)$, a "strong electric field" case.

equilibrium solutions are: $\phi \equiv 0$ — a stable one, $\phi \equiv 1$ — an unstable one. This case can be conventionally called a case of "strong electric field". This means that the electric field is sufficiently strong and any state arbitrarily close to the completely undamaged one (i.e., any state close to $\phi \approx 1$) evolves towards the completely damaged state $\phi = 0$. Essentially this is the case where the completely damaged state develops from arbitrarily small perturbations of the completely undamaged equilibrium solution.

In all the three cases stability of the equilibrium solution $\phi \equiv 0$ is defined by the higher order derivatives of $\chi(\phi)$.

## 4. The finite-difference scheme

In this section, we present a finite-difference scheme for solving equation (9) in the domain $[0,W]_x \times [0,+\infty)_t$. The equation is subjected to initial conditions (10) and boundary conditions (11).

Consider a regular mesh with a time step $\tau$ and a spatial step $h$. Let $W = Nh$ with $N$ being the number of nodes. The nodes of the spatiotemporal grid are given by $(jh, k\tau)$, $j = \overline{0,N}$, $k \in \mathbb{N}_0$. Define by $\phi_j^k$ the value of the mesh function $\phi$ at the node $(jh, k\tau)$. Then, the finite-difference approximations is

$$\frac{1}{m}\frac{\phi_j^{k+1} - \phi_j^k}{\tau} = \frac{1}{2}K_\phi^2 \varepsilon'\left(\phi_j^k\right) + \frac{\Gamma}{l^2} f'\left(\phi_j^k\right) + \frac{\Gamma}{2}\frac{\phi_{j+1}^k - 2\phi_j^k + \phi_{j-1}^k}{h^2}, \tag{22}$$

or, in the explicit form,

$$\phi_j^{k+1} = \phi_j^k + m\tau\left(\frac{1}{2}K_\Phi^2 \varepsilon'\left(\phi_j^k\right) + \frac{\Gamma}{l^2} f'\left(\phi_j^k\right) + \frac{\Gamma}{2}\frac{\phi_{j+1}^k - 2\phi_j^k + \phi_{j-1}^k}{h^2}\right), \tag{23}$$

$$j = \overline{1, N-1}, \quad k \in \mathbb{N}_0;$$

$$\phi_j^0 = \phi_0(jh); \quad \phi_0^k = \phi_l(k\tau); \quad \phi_N^k = \phi_r(k\tau). \tag{24}$$

It is easy to see that the scheme has the first order of approximation in time and the second order of approximation in spatial terms.

To study properties of scheme (23), (24), the linear theory can be used (see, e.g., [16, Chapter 10] or [17, Chapter IX]). The central result of the theory states, in a somewhat simplified form, that if a finite-difference scheme is stable and approximates a continuous problem then the solution of the finite-dimensional problem converges to the solution of the continuous one with order no lower than the order of approximation.

To apply this result for nonlinear setting (23), (24), we proceed as follows: (i) linearize equation (22) for a fixed $\phi$ and then (ii) apply the spectral stability argument [16] to the derived linearized equation. As the stability criteria are satisfied for the linearized equation, stability should be expected for the complete, nonlinear, problem. In this case, the convergence of the approximate solution should be expected as well — since the finite-difference problem is stable and approximates the continuous one. The results of such non-rigorous analysis will be further confirmed by numerical computations in the fully nonlinear setting.

### 4.1. Stability estimate

In this section, we derive a stability condition for finite-difference scheme (23), (24), using the so-called principal of "frozen coefficients" (see, e.g., [16]). Let $\phi_j^k$ and $\phi_j^k + \delta_j^k$ be solutions of finite-difference equation (22). Substitute $\phi_j^k + \delta_j^k$ into (22) to obtain:

$$\frac{1}{m}\frac{\left(\phi_j^{k+1}+\delta_j^{k+1}\right)-\left(\phi_j^k+\delta_j^k\right)}{\tau} = \frac{1}{2}K_\Phi^2\left[\varepsilon'\left(\phi_j^k\right)+\varepsilon''\left(\phi_j^k\right)\delta_j^k+o\left(\delta_j^k\right)\right]+$$

$$+\frac{\Gamma}{l^2}\left[f'\left(\phi_j^k\right)+f''\left(\phi_j^k\right)\delta_j^k+o\left(\delta_j^k\right)\right]+\frac{\Gamma}{2}\frac{\left(\phi_{j+1}^k+\delta_{j+1}^k\right)-2\left(\phi_j^k+\delta_j^k\right)+\left(\phi_{j-1}^k+\delta_{j-1}^k\right)}{h^2}.$$

Linearizing this equation around $\phi_j^k = P$, assuming that perturbations $\delta_j^k$ are small and taking into account that $\phi_j^k$ is a solution of the finite-difference problem, we obtain:

$$\delta_j^{k+1} = \delta_j^k + m\tau\left(\frac{1}{2}K_\Phi^2\varepsilon''(P)\delta_j^k + \frac{\Gamma}{l^2}f''(P)\delta_j^k + \frac{\Gamma}{2}\frac{\delta_{j+1}^k - 2\delta_j^k + \delta_{j-1}^k}{h^2}\right). \tag{25}$$

We now apply spectral stability analysis to the derived equation for perturbations. Let $\delta_j^k = \lambda(\theta)^k \cdot \exp(\imath j\theta)$, $\imath^2 = -1$. Substituting this representation into (25), one obtains:

$$\lambda(\theta) = 1 + m\tau\left(\frac{1}{2}K_\Phi^2\varepsilon''(P) + \frac{\Gamma}{l^2}f''(P) + \frac{\Gamma}{2}\frac{\exp(\imath\theta) - 2 + \exp(-\imath\theta)}{h^2}\right),$$

or

$$\lambda(\theta) = 1 + m\tau\left(\frac{1}{2}K_\Phi^2\varepsilon''(P) + \frac{\Gamma}{l^2}f''(P) - \frac{2\Gamma}{h^2}\sin^2\frac{\theta}{2}\right). \tag{26}$$

According to the spectral stability argument, a time step $\tau = \tau(h)$ provides stability of the scheme in the domain $[0,W]_x \times [0,T]_t$ with $T < +\infty$ as $\tau, h \to 0$ if there exists $C > 0$ such that for an arbitrary $\theta$ it holds $|\lambda(\theta)| \leqslant \exp(C\tau)$. Note that it is also possible to use a more strict condition $|\lambda(\theta)| \leqslant 1 + C\tau$ here. If for an arbitrary $\theta$ it holds $|\lambda(\theta)| \leqslant 1$ then stability will be provided also for an unbounded time interval, i.e., for $[0,W]_x \times [0,+\infty)_t$. Strictly speaking, the spectral argument does not provide a sufficient stability condition; however, stability should be expected in practice.

First, consider expression (26) for $P = 0$. We have $f''(0) = 0$, $\varepsilon''(0) = 0$, and equation (26) takes the form of

$$\lambda(\theta) = 1 - \frac{2\tau m\Gamma}{h^2}\sin^2\frac{\theta}{2}.$$

Hence, for an arbitrary $\theta$ it holds $|\lambda(\theta)| \leqslant 1$ if and only if

$$\tau \leqslant \frac{h^2}{m\Gamma} \tag{27}$$

As condition (27) is satisfied, one can expect stability of the scheme while the solution describes an almost completely damaged state $\phi \approx 0$ in the domain $[0,W]_x \times [0,+\infty)_t$

Note that under condition (27) one also can expect stable computations for $[0,W]_x \times [0,T]_t$ for an arbitrary value $P \in [0,1]$. In this case the following is true:

$$\left|\lambda(\theta)\right| \leqslant \left|1 - \frac{2\tau m\Gamma}{h^2}\sin^2\frac{\theta}{2}\right| + m\tau\left|\frac{1}{2}K_\Phi^2\varepsilon''(P) + \frac{\Gamma}{l^2}f''(P)\right| \leqslant 1 + m\tau\left|\frac{1}{2}K_\Phi^2\varepsilon''(P) + \frac{\Gamma}{l^2}f''(P)\right|.$$

Hence, there exists $C$ such that $\left|\lambda(\theta)\right| \leqslant 1 + C\tau$ holds, — since $\varepsilon''(\phi)$ and $f''(\phi)$ are continuous on $[0,1]$. It should be noted that, despite such versatility, estimate (27) is poorly applicable in practice and requires clarification, which will be done later.

We now consider expression (26) at the value $P = 1$. Note that $f''(1) < 0$, $\varepsilon''(1) > 0$. We see that for $\left(K_\Phi^2/2\right)\varepsilon''(1) + \left(\Gamma/l^2\right)f''(1) \leqslant 0$ it is possible to achieve $\left|\lambda(\theta)\right| \leqslant 1$ with demanded sufficiently small values of $\tau$ and the condition $\tau \leqslant h^2/(2m\Gamma)$, similar to the one for (27). Substituting $f''(1) = -12$, $\varepsilon''(1) = 12\varepsilon_0/(1+\delta)^2$ (see (12)), we obtain

$$\frac{K_\Phi^2 l^2 \varepsilon_0}{2\Gamma(1+\delta)^2} \leqslant 1. \tag{28}$$

So, under condition (28) it is expected that there exist such values of $\tau$ and $h$ that the difference scheme is stable for $\phi \approx 1$ and $T = +\infty$. Naturally condition (28) is equivalent to stability condition (19) for the equilibrium state $\phi \equiv 1$ of equation (9).

## 4.2. Improved stability estimate

In the previous section, form the analysis of equation (26) stability condition (27) was derived for finite-difference scheme (23), (24) for $\phi \approx 0$. The assumption of its usefulness is based on the fact that a typical "'natural" solution of the model has a form of transition process from the undamaged state $\phi = 1$ to the completely damaged state $\phi = 0$ occurring in a finite time interval and then staying in the damaged state $\phi \approx 0$ forever.

Nevertheless, the performed analysis of equation (26) is not sufficient at $\phi = 0$. Indeed, it was used that at $\phi = 0$ $\varepsilon''(0) = 0$ (see expression (12)), — but it was not accounted that $\varepsilon''(\phi)$ grows fast and reaches large values for small $\delta \approx 0$ (see Fig. 4). This means that the equations of the model are stable at $\phi = 0$ but can be unstable in a small neighbourhood of $\phi = 0$. Such situation is not satisfactory and we now try to improve the obtained stability estimate.

To proceed let us estimate extremums of $\varepsilon''(\phi)$ in the neighbourhood of $0$. First, find the zeros of $\varepsilon'''(\phi)$. We have

$$\varepsilon''' = \varepsilon_0 \frac{-6(f')^3 + 6(f+\delta)f'f'' - (f+\delta)^2 f'''}{(f+\delta)^4}, \tag{29}$$

form where:

$$\varepsilon'''(\phi) = -6(f')^3 + 6(f+\delta)f'f'' - (f+\delta)^2 f''' = 0,$$

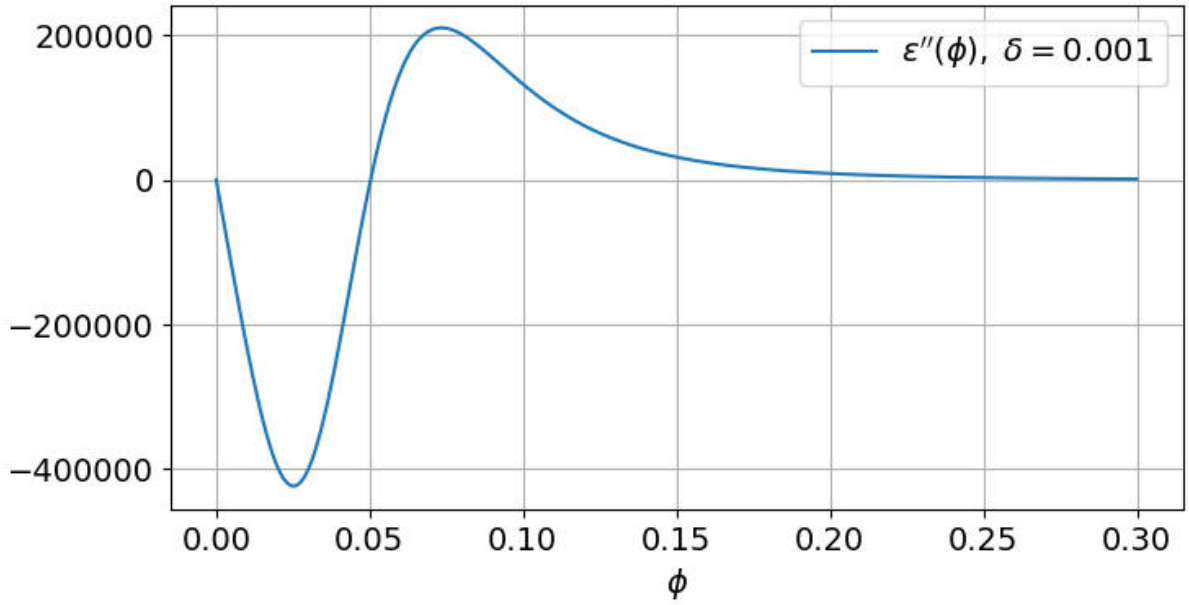


Figure 4. Typical behavior of $\varepsilon''(\phi)$ in the vicinity of $0$.

or, taking $(1)$ into account:

$$-3\cdot 12^2(1-\phi)^3+36\left(4-3\phi+\frac{\delta}{\phi^3}\right)(1-\phi)(2-3\phi)-\left(4-3\phi+\frac{\delta}{\phi^3}\right)^2(1-3\phi)=0.$$

Let $\delta_n\to+0$ and $\phi_n\to+0$ such that $\delta_n/\phi_n^3$ is bounded. Then:

$$-3\cdot 12^2\cdot 1^3+36\left(4+\frac{\delta_n}{\phi_n^3}\right)\cdot 1\cdot 2-\left(4+\frac{\delta_n}{\phi_n^3}\right)^2\cdot 1\to 0,$$

$$\left(4+\frac{\delta_n}{\phi_n^3}\right)^2-72\left(4+\frac{\delta_n}{\phi_n^3}\right)+3\cdot 12^2\to 0.$$

Hence, the sequence $4+\delta_n/\phi_n^3$ has at most two partial limits $\xi_+$ and $\xi_-$ being zeros of the equation $\xi^2-72\xi+432=0$. To the first zero $\xi_+=36+12\sqrt{6}$ corresponds

$$\phi_+=\frac{1}{\sqrt[3]{32+12\sqrt{6}}}\sqrt[3]{\delta_n}\approx\frac{1}{3.945}\sqrt[3]{\delta_n};$$

to the second zero $\xi_-=36-12\sqrt{6}$ corresponds

$$\phi_-=\frac{1}{\sqrt[3]{32-12\sqrt{6}}}\sqrt[3]{\delta_n}\approx\frac{1}{1.376}\sqrt[3]{\delta_n}.$$

From here it can be seen that as $\delta\to+0$ the function $\varepsilon'''(\phi)$ has two zeros in the neighbourhood of $0$:

$$\phi_\pm=\frac{1}{\sqrt[3]{32\pm 12\sqrt{6}}}\sqrt[3]{\delta}\left[1+o(1)\right]. \tag{30}$$

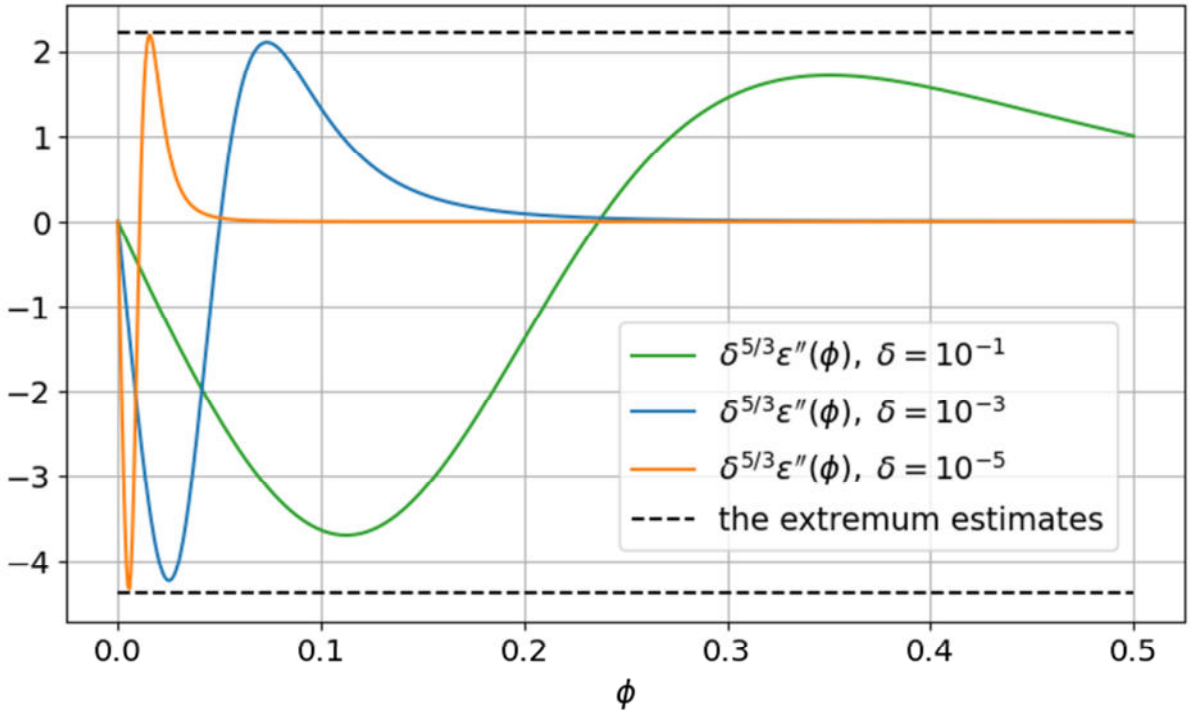


Figure 5. Qualitative behavior of $\delta^{5/3}\varepsilon''(\phi)$ for small values of $\delta$.

We now estimate $\varepsilon''(\phi)$ at $\phi_{\pm}$ as $\delta \to +0$. Let $\phi = (1/c)\sqrt[3]{\delta}$, $c \in \mathbb{R}$. Then:

$$\varepsilon'' = \varepsilon_0 \frac{24c^5\left(8-c^3\right)}{\left(4+c^3\right)^3}\delta^{-5/3}\left[1+o(1)\right],$$

and:

$$\varepsilon''(\phi_+) \approx -4.378\varepsilon_0\delta^{-5/3}; \quad \varepsilon''(\phi_-) \approx 2.216\varepsilon_0\delta^{-5/3}. \tag{31}$$

The derived estimates are shown as black dashed lines in Fig. 5.

Now, to derive a new stability estimate, we consider equation (26) at $\phi = \phi_+$. Note that $\varepsilon''(\phi_+) \approx -4.4\varepsilon_0\delta^{-5/3}$. The term inside braces in (26) is negative since $\delta$ is small and $\varepsilon''(\phi_+)$ is negative and large in its absolute value. Therefore $f''(\phi_+) > 0$ can be estimated as 0 — such estimate makes the inequality stronger. Then, from inequality (26) it follows that

$$\lambda(\theta) = 1 + m\tau\left(-\frac{2.2K_\Phi^2\varepsilon_0}{\delta^{5/3}} - \frac{2\Gamma}{h^2}\sin^2\frac{\theta}{2}\right).$$

Condition $|\lambda(\theta)| \leqslant 1$ is satisfied for an arbitrary $\theta$ if and only if

$$\tau \leqslant \frac{1}{m}\left(\frac{1.1K_\Phi^2\varepsilon_0}{\delta^{5/3}} + \frac{\Gamma}{h^2}\right)^{-1}. \tag{32}$$

The numerical experiments described in the next sections indicate that a stronger version of estimate (32) is also valid (note the doubled denominator):

$$\tau \leqslant \frac{1}{2m}\left(\frac{K_\Phi^2 \varepsilon_0}{\delta^{5/3}} + \frac{\Gamma}{h^2}\right)^{-1}. \tag{33}$$

Finally, a more simple estimate not weaker than (33) is:

$$\tau \leqslant \frac{1}{4m}\min\left(\frac{\delta^{5/3}}{K_\Phi^2 \varepsilon_0},\ \frac{h^2}{\Gamma}\right). \tag{34}$$

Note that derived stability estimate (33) for finite-difference scheme (23), (24) includes all the parameters of equation (9), except $l$. Notably, this is the only parameter of the model which has somehow artificial nature and can not be related directly to the underlying physics.

# 5. Numerical studies

In this section, we present some numerical results obtained using finite-difference scheme (23), (24), presented above. The main goal of the simulations is to confirm theoretical stability estimates derived for the model itself and its approximations, i.e., convergence and stability of the finite-difference scheme (see condition (33)) and stability properties of the equilibrium solutions described in section 3. In addition, we will check temporal behavior of the total free energy of the system.

## 5.1. A typical solution

Let us set the parameters of equation (9) as follows:

$$\varepsilon_0 = 0.2,\ \ \delta = 0.04,\ \ l = 1.0,\ \ \Gamma = 1.0,\ \ m = 0.5,\ \ K_\Phi = 4.8. \tag{35}$$

Note that this set of parameters corresponds to a "strong electric field" case, see (21).

The equation is solved in the spatiotemporal domain

$$\bar{\Omega} = [0, W]_x \times [0, T]_t,\ \ W = 5,\ \ T = 1. \tag{36}$$

The boundary conditions are defined as follows:

$$\phi(0,t) = 1,\ \ \phi(W,t) = 1,$$

$$\phi(x,0) = \phi_0(x) = \begin{cases} 1, & \text{if } x \leqslant 2.25 \text{ or } x \geqslant 2.75; \\ 1 - 0.025 \cdot \left[1 + \cos(4\pi x)\right], & \text{if } 2.25 < x < 2.75. \end{cases} \tag{37}$$

Note that $\phi_0(x)$ is a twice differentiable function everywhere except a finite number of points; moreover, its second derivative is bounded.

Let $N_x$ be the number of mesh steps on $[0, W]_x$ (the number of nodes is, respectively, $N_x + 1$); $N_t$ be the number of mesh steps on $[0, T]_t$. The spatial and temporal mesh step sizes are given by $h = W / N_x$, $\tau = T / N_t$.

In Fig. 6 the typical solution is presented. It is easy to see gradual evolution of the breakdown channel (identified as a spatial domain where the medium is damaged) developing from a sufficiently small perturbation of the initial, completely undamaged, state. Approximately at the time $t = 0.55$ the medium in the breakdown channel becomes completely damaged: the values of $\phi$ in the neighborhood of $x = 2.5$ get closed to the zero value. Note that for $t \in (0.3,\ 0.55)$ the breakdown

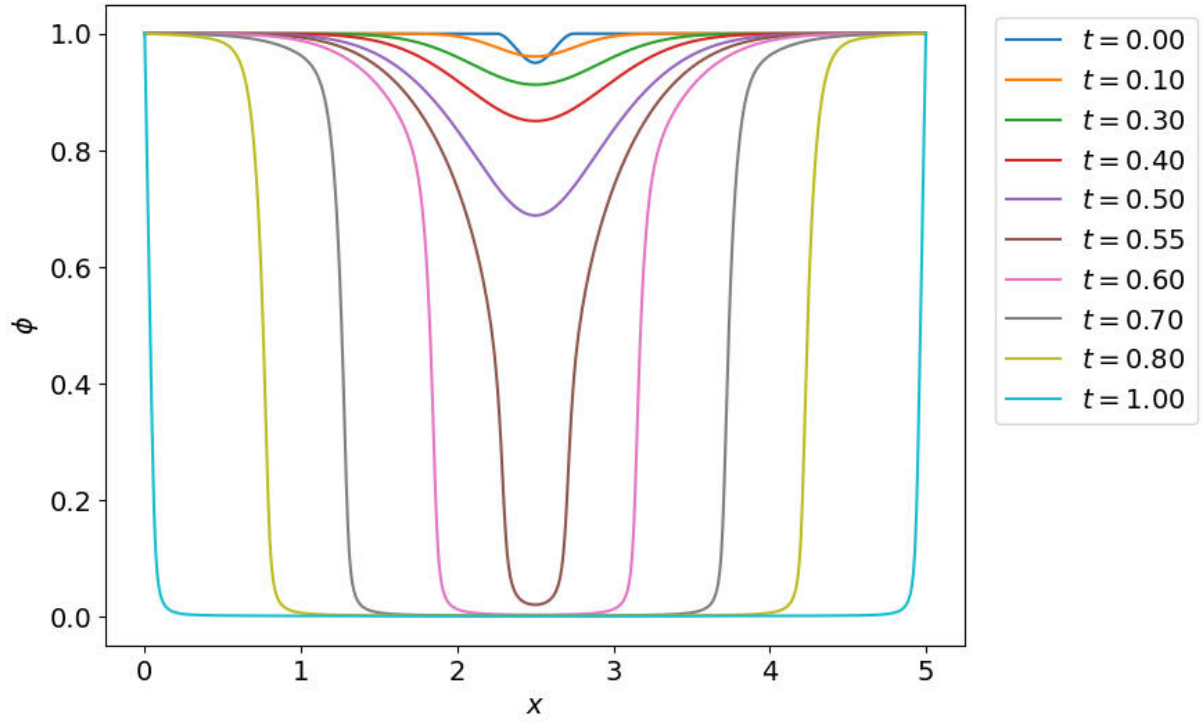


Figure 6. The typical solution of the problem, $N_x = 10^3$, $N_t = 10^5$.

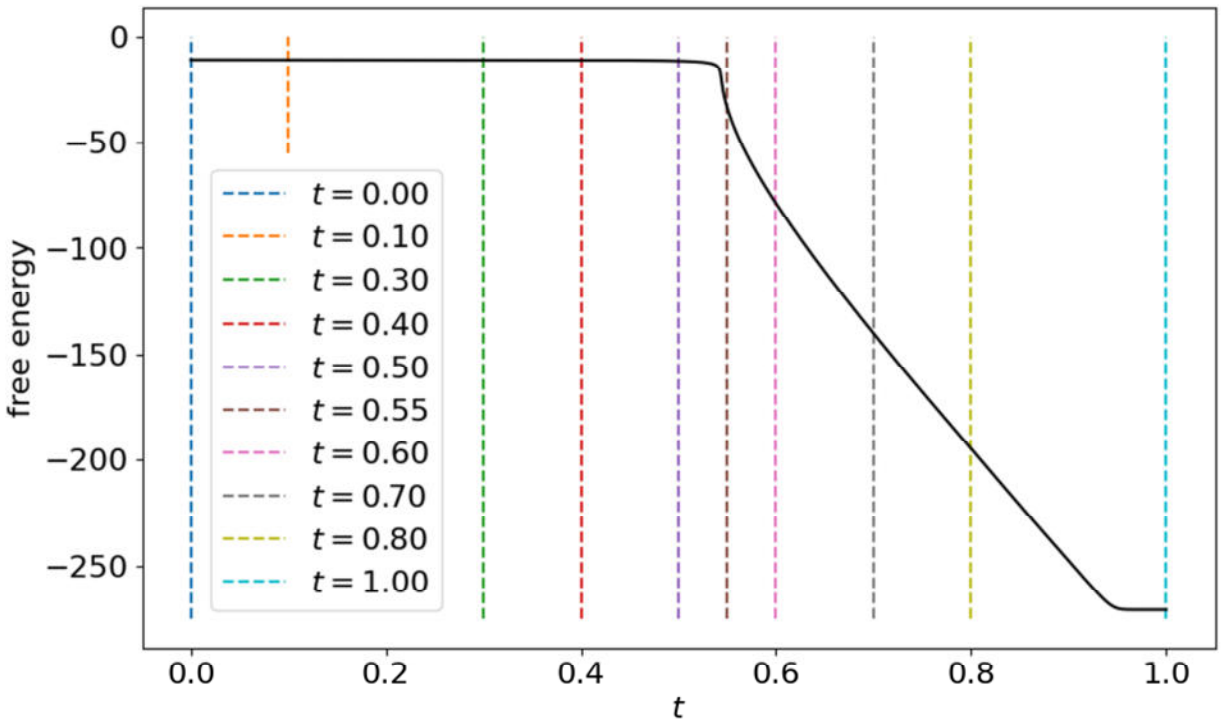


Figure 7. The free energy evolution.

channel (identified as a spatial domain where $\phi$ essentially differs from 1) practically does not change its width. The width is approximately equal to $2l$, as is supposed in the model. On the

contrary, for $t > 0.55$, when $\phi$ reaches its minimal values, the channel grows wide with almost constant velocity.

## 5.2 Evolution of the free energy

In the model under consideration, the free energy of the system is given by (2) with its density given by (3). In the finite-dimensional setting, the terms in (3) can be approximated in an obvious way. The only essential addition we need to mention is the approximation of the first derivative, i.e., $\partial_h \phi_i^j / \partial_h x$. Further, the simplest approach is considered, which uses the standard first-order approximation of $\partial_h \phi_i^j / \partial_h x$.

To simulate the solution of the system, we use the same finite-difference scheme, initial and boundary conditions as in the previous section.

The results are given in Fig. 7, where the dependence $\Pi = \Pi(t)$ is shown. The colored vertical dashed lines correspond to the same time moments as in Fig. 6. It is interesting to note that for $t < 0.5$ the free energy $\Pi$ is almost constant; further, for $t > 0.5$ it starts to decrease sufficiently fast until $t \approx 0.55$. Later, after $t = 0.6$ the energy decreases linearly until the medium is completely damaged.

It can be seen from the derivation of (5) and (6), that the system tends to minimize its free energy during its evolution. Due to this, the correct monotone decrease of the free energy is of the crucial importance for the simulation to be qualitatively correct. We do not provide a strict proof of the correct behavior of the scheme here (which is an important but standalone task), but rather check it in the performed simulations. This means that under the given parameters of the model and discretization, the scheme is gradient-stable (or, what is the same, energy-stable).

## 5.3. Stability of the scheme

In this section, we check stability estimate (33) of the finite-difference scheme.

Let the model parameters be defined according to (35) and (36), the boundary conditions be given by (37). We assume by convention that the scheme is unstable as soon as the simulation finishes abnormally with floating point overflow due to division by zero (e.g., in expression (1) for $\varepsilon(\phi)$ at $f(\phi) = -\delta$) or with the values of $\phi$ going to infinity (as in overflow of variables of the type double). We increase $N_x$ and $N_t$, keeping the information about pairs of values at which stable approximation turns into unstable one. Plotting these values, we can depict the stability region of the scheme on the $N_x$ - $N_t$ plane. Such plot is presented in Fig. 8 together with the theoretical boundary given by stability estimate (33).

Numerical experiment demonstrates that estimate (33) is successful and sufficiently sharp: the theoretical and experimental stability boundaries follow each other and are relatively closed. Moreover, the theoretical curve lies above the experimental one, which means that the theoretical estimate is stricter than the experimental one. Actually, this is the reason to divide the right-hand side of original estimate (32) by two.

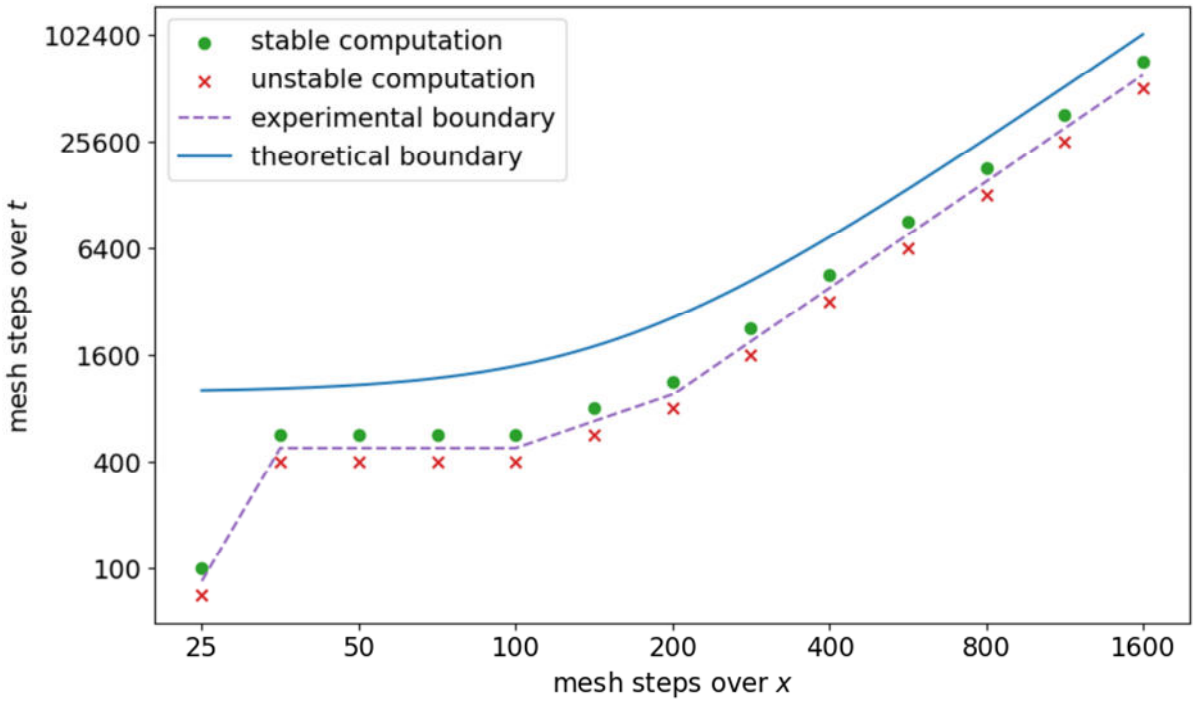


Figure 8. The theoretical and experimental stability boundaries.

### 5.4. Convergence

The approximation property of finite-difference scheme (23), (24) solving the problem (9), (10), (11) is obvious. Stability of the scheme is provided by theoretical estimate (33), which was verified by numerical experiments. We now check convergence of the finite-difference solution.

Define the $\|\cdot\|_C$ and $\|\cdot\|_2$ norms as

$$\| f \|_C = \max_{(x,t)\in\bar{\Omega}} |f(x,t)|; \qquad \| f \|_2 = \sqrt{\int_{\bar{\Omega}} f^2(x,t)\,dxdt}$$

in space $C_2(\bar{\Omega})$ of twice differentiable functions in the closed spatiotemporal domain $\bar{\Omega} = [0,W]_x \times [0,T]_t$.

Consider a computational mesh $\Omega_{h,\tau} \subset \bar{\Omega}$ together with some dependence $\tau = \tau(h)$. Restricting functions from $C_2(\bar{\Omega})$ on the mesh $\Omega_h = \Omega_{h,\tau(h)}$, we obtain space of mesh functions $C_2(\bar{\Omega})_h$. The functional norms in space $C_2(\bar{\Omega})_h$ can be defined as

$$\| f_j^k \|_C = \max_{(j,k)\in\Omega_h} |f_j^k|; \qquad \| f_j^k \|_2 = \sqrt{h\tau \sum_{(j,k)\in\Omega_h} (f_j^k)^2}.$$

Now consider the results of numerical experiments. Convergence will be analysed using the norms $\|\cdot\|_C$ and $\|\cdot\|_2$ in space of mesh functions defined above. Since the analytical solution of the problem is not known, a comparison will be performed using a sequence of approximate solutions against the solution obtained using the finest mesh. To compute the difference between two finite-difference solutions, we restrict the solution obtained using the finer mesh on the more coarse one, ignoring the fine solution values at the respective mesh nodes.

To proceed, we set the parameters of the model as described above, see (35), (36). Let $N_x = W/h$ be the number of mesh steps in the spatial domain, $N_t = T/\tau$ be the number of mesh steps in the time domain. In all further simulations stability condition (33) is satisfied.

First, we set $N_x = 200$ and perform a sequence of simulations with gradually increasing $N_t$, doubling it at each step. The comparison of the solutions with the one obtained for $N_t = 204800$ is shown in Fig. 9. The results clearly show that the scheme produces solutions with first-order convergence rate to the "exact" one over time $t$, which confirms the theoretical estimates. So, the scheme has $\mathcal{O}(\tau)$ accuracy.

Second, we set $N_t = 204800$ and perform a sequence of simulations with increasing $N_x$, again, doubling it at each step. The comparison of the solutions with the one obtained for $N_x = 1600$ is shown in Fig. 10. The results clearly show that the scheme produces solutions with second-order convergence rate to the "exact" one over spatial variable $x$, which confirms the theoretical estimates. So, the scheme has $\mathcal{O}(h^2)$ accuracy.

We now refine both $N_x$ and $N_t$ in such a way that for the used values of $h$ and $\tau$ as $h, \tau \to 0$ it holds stability condition (33). For the parameters of the model defined above, one can set $N_t = 0.08 \cdot N_x^2$. The errors between a sequence of approximate solutions and the reference one are computed in the same way as earlier; the results are presented in Fig. 11. As it was expected, the convergence order is $\mathcal{O}(\tau + h^2) = \mathcal{O}(\tau)$, as soon as the spatial and temporal discretization parameters are related as described above.

Note that in the first two experiments, the limiting solution was not an actual solution of the differential problem since only one discretization parameter was tending to its limiting value. The second one had a fixed value and, therefore, the reference numerical solution always had an irremovable approximation error. In the third experiment, under assumption that the scheme is stable, the numerical solutions converge to the solution of the initial differential problem (9), (10), (11).

## 5.5 Stability of the equilibrium states

Earlier we studied equilibrium solutions $\phi \equiv C$ of equation (9). Their number and stability types are defined by the value of $\xi$, given by (21).

Define the parameters of the model according to (35) and (36), — except the value of $K_\Phi$, which will be defined later. As the initial condition, we set a perturbation of the constant equilibrium state: $\phi(x,0) = C + A\cos(\omega x)$ ; $\phi(0,t) = \phi(0,0)$ , $\phi(W,t) = \phi(W,0)$ . The amplitude $A$ is considered to be relatively small, i.e., $A \sim 0.01$. The numbers of computational steps are given by $N_x = 800$ and $N_t = 51200$.

If an equilibrium state is stable then for an arbitrary $\omega$ the perturbation in the initial condition decays; if an equilibrium state is unstable then there exists some $\omega_0$ such that for any $\omega < \omega_0$ the perturbation increases over time.

Let us set $K_{\Phi,1} = 0$, $K_{\Phi,2} = 1.1$, $K_{\Phi,3} = 4.8$. For $\delta = 0.04$, as it was defined above, one has

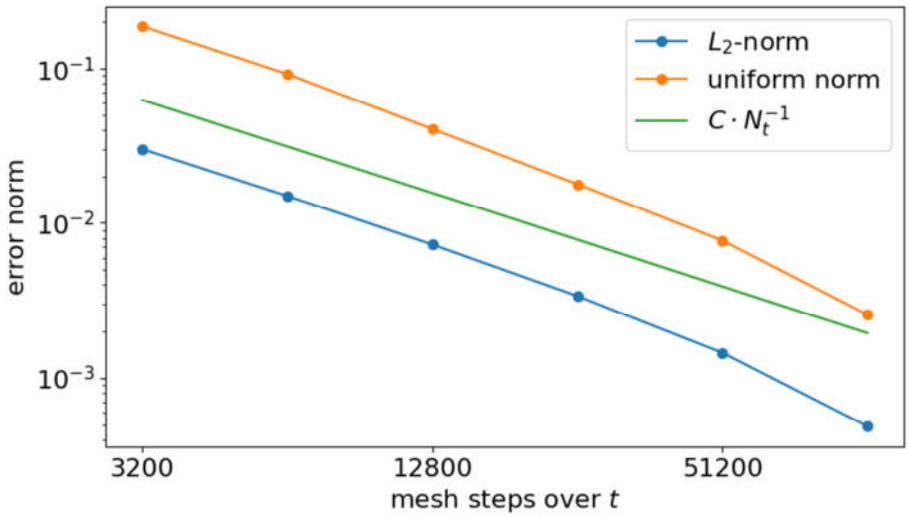


Figure 9. The error norm for the fixed $N_x = 200$.

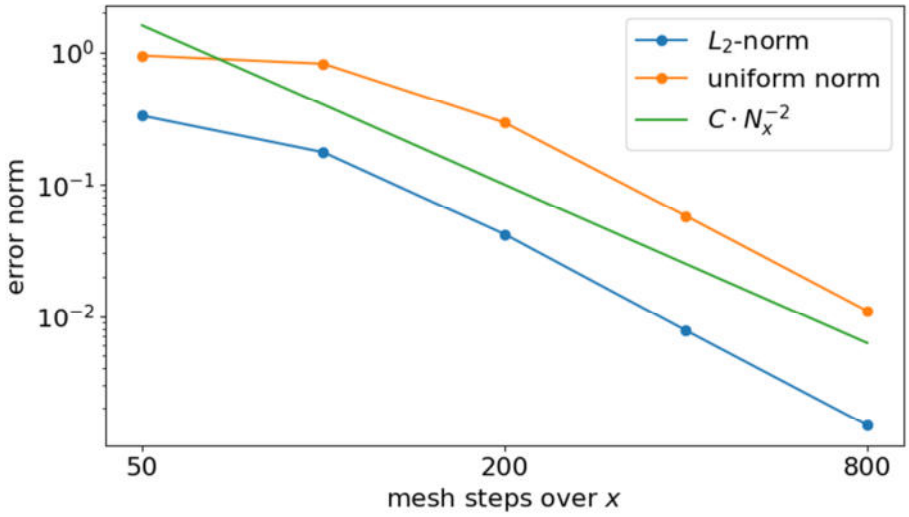


Figure 10. The error norm for the fixed $N_t = 204800$.

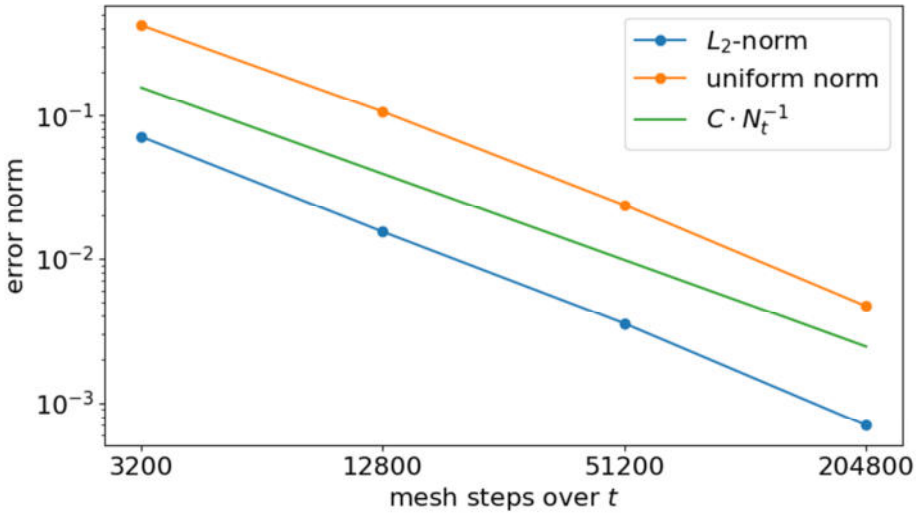


Figure 11. The error norm for $N_t = 0.08 \cdot N_x^2$.

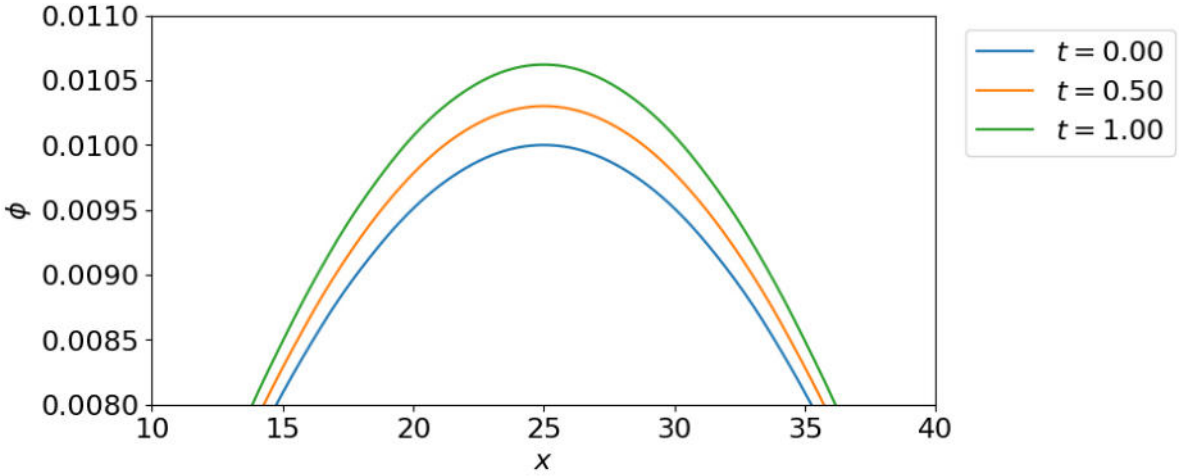


Figure 12. A "weak electric field" case: the perturbed equilibrium state $\phi \equiv 0$, unstable.

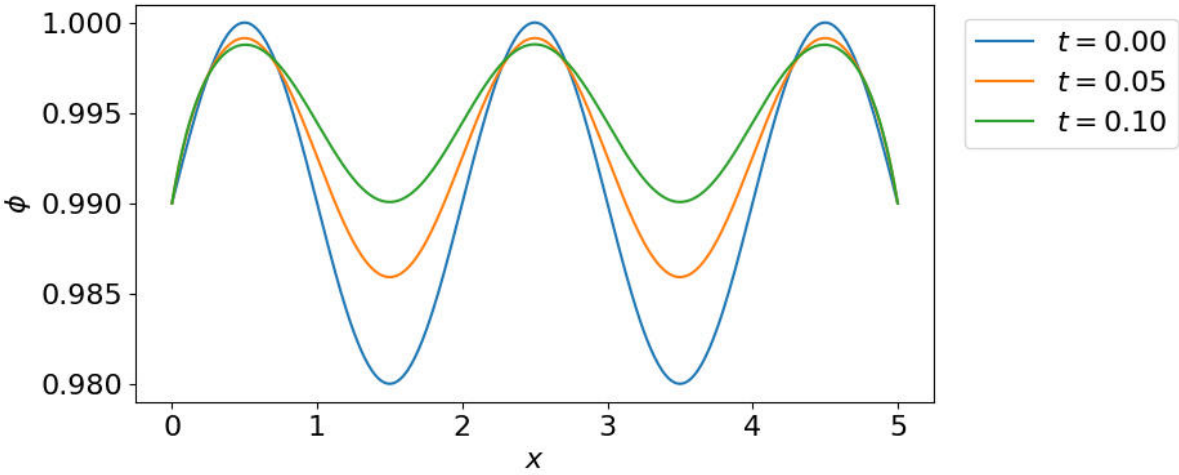


Figure 13. A "weak electric field" case: the perturbed equilibrium state $\phi \equiv 1$, unstable.

$\xi_1 = 0 < \delta^2$, $\xi_2 = 0.121 \in (\delta^2, (1+\delta)^2)$, $\xi_3 = 2.304 > (1+\delta)^2$.

First, consider $K_{\Phi,1} = 0$, $\xi_1 < \delta^2$ — this is a case of "weak electric field". In this case the system has two equilibrium states: $\phi \equiv 0$ — a unstable one and $\phi \equiv 1$ — a stable one. On the Figs. 12 and 13 it is easy to see theoretically predicted evolution of the solution: for $C = 0$ there is a perturbation growth, for $C = 1$ — a perturbation decrease. For the value $C = 0$ the derivative of the function $\chi(\phi)$ (see (20)) vanishes, therefore, to observe growth of the perturbation, it is necessary to define sufficiently small values of $\omega$, which, in turn, provides a sufficiently small value of $\partial^2\phi / \partial x^2$. Note that in the experiment with $\phi \equiv 1$, we take $C = 1 - A$ in order to keep the values of $\phi$ below 1.

Now consider $K_{\Phi,2} = 1.1$, $\xi_2 \in (\delta^2, (1+\delta)^2)$ — i.e., a case of "medium electric field". In this case the system has three equilibrium states: $\phi \equiv 0$ — a stable one, $\phi \equiv C_3 \approx 0.5$ — an unstable one ($C_3$ is the zero of $\chi(\phi)$ in the interval $(0,1)$), $\phi \equiv 1$ — a stable one. Evolution of the perturbed

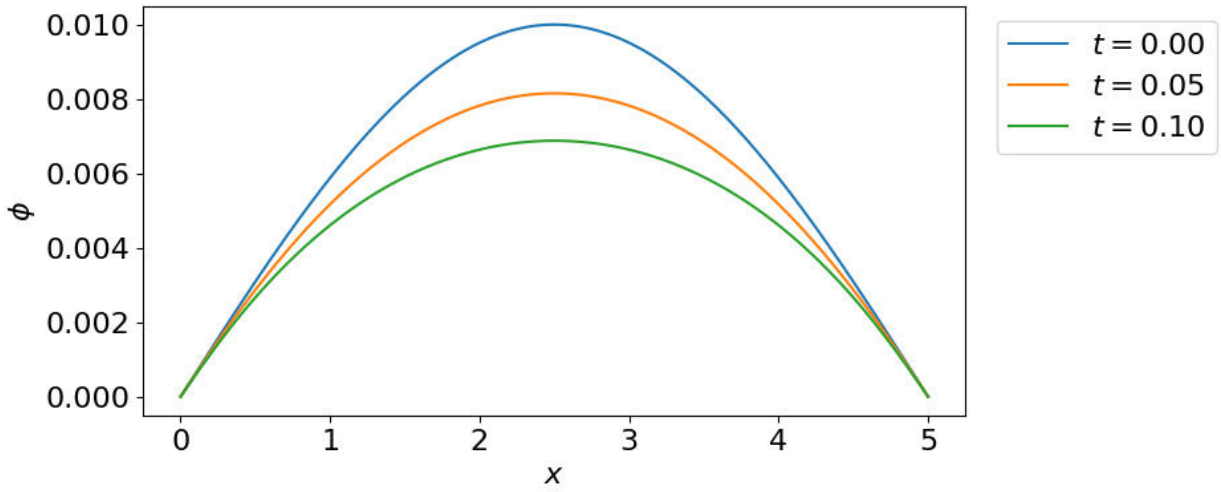


Figure 14. A "medium electric field" case: the perturbed equilibrium state $\phi \equiv 0$, stable.

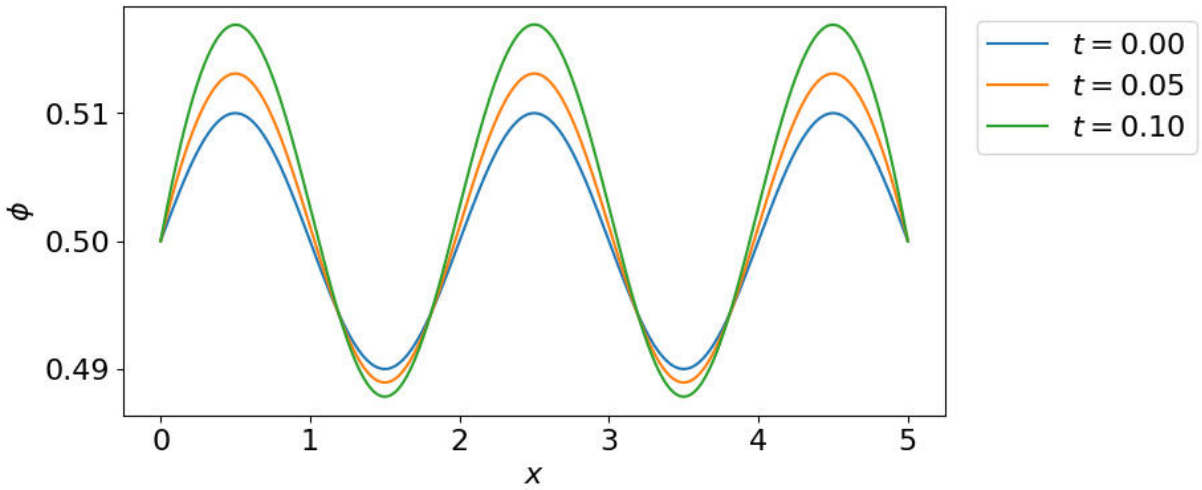


Figure 15. A "medium electric field" case: the perturbed equilibrium $\phi \equiv C_3 \approx 0.5$, unstable.

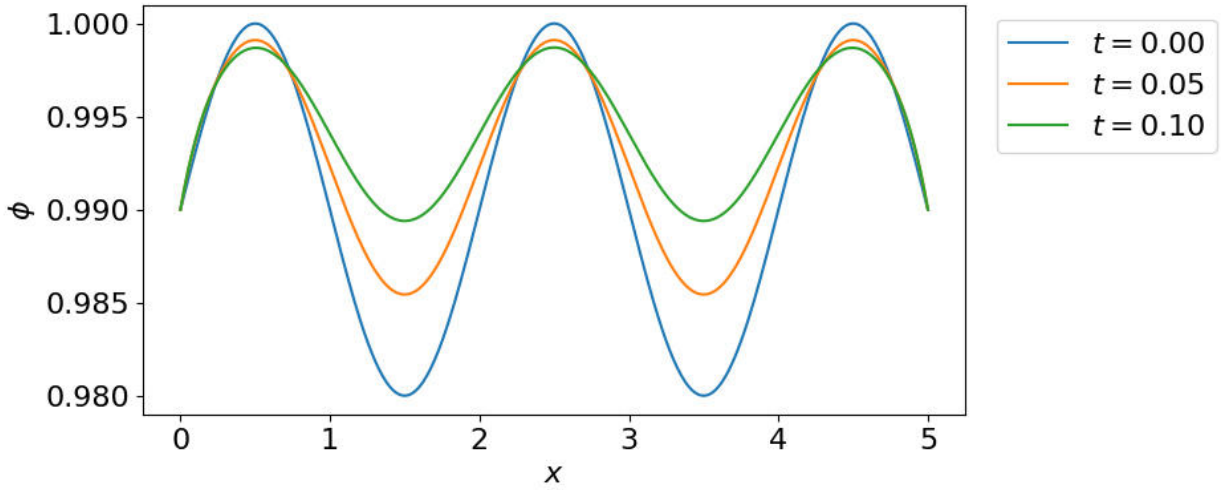


Figure 16. A "medium electric field" case: the perturbed equilibrium state $\phi \equiv 1$, stable.

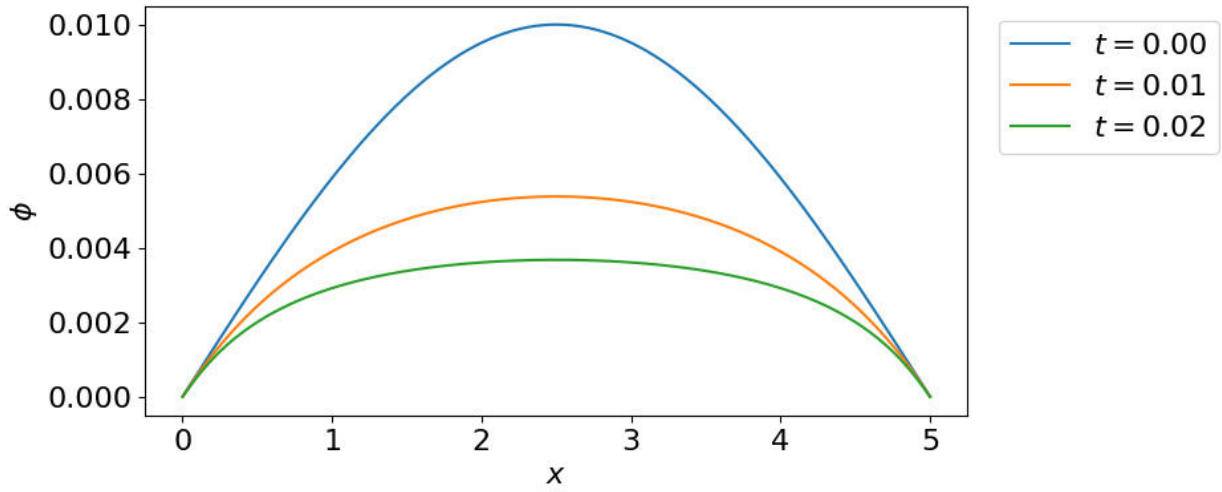


Figure 17. A "strong electric field" case: the perturbed equilibrium state $\phi \equiv 0$, stable.

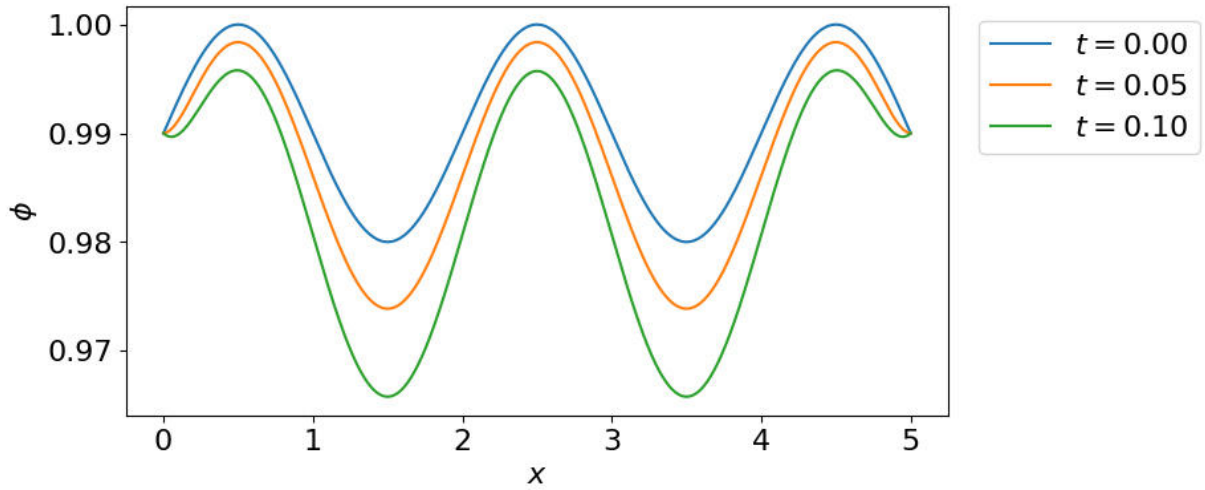


Figure 18. A"strong electric field" case: the perturbed equilibrium state $\phi \equiv 1$, unstable.

solution is shown in Figs. 14, 15 and 16. As it can be seen, the observed behavior is in accordance with the theoretically predicted one.

Finally, consider the case of $K_{\Phi,3} = 4.8$, $\xi_3 > (1+\delta)^2$, corresponding to a "strong electric field" case. The system has two equilibrium states: $\phi \equiv 0$ (stable) and $\phi \equiv 1$ (unstable). Evolution of the perturbed solution is shown in Figs. 17 and 18. As in other considered cases, the results coincide with the theoretical predictions.

## 6. Conclusion

In this paper we study the stability properties of the phase-field model for the electrical breakdown channel evolution. The central result is the classification of the equilibrium solutions of the model and their stability. From a practical point of view, these results allow to make meaningful conclusions regarding the qualitative and quantitative properties of the model. Particularly, it was shown under what conditions small perturbations of the intact medium develop into a channel-like

structure typical for the electrical breakdown process.

Besides this, the simple explicit finite-difference scheme solving the problem in the spatially one-dimensional setting is considered. The main question addressed here is about stability conditions guaranteeing the correctness of simulations. Deep connections between the stability conditions of the model and the ones of the finite-difference scheme are shown. The presented results of numerical simulations confirm the predictions of the model theoretical analysis.

## References


1. Dissado L., Fothergill J. Electrical Degradation and Breakdown in Polymers. — London : Peter Peregrinus, 1992.
2. Pitike K. C., Hong W. Phase-field model for dielectric breakdown in solids // Journal of Applied Physics. — 2014. — Jan. — Vol. 115, no. 4. — P. 044101. — DOI: 10.1063/1.4862929. — URL: https://doi.org/10.1063/1.4862929.
3. Lamorgese A. G., Molin D., Mauri R. Phase Field Approach to Multiphase Flow Modeling // Milan Journal of Mathematics. — 2011. — Dec. — Vol. 79, no. 2. — P. 597–642. — DOI: 10.1007/s00032-011-0171-6. — URL: https://doi.org/10.1007/s00032-011-0171-6.
4. Kim J. Phase-Field Models for Multi-Component Fluid Flows // Communications in Computational Physics. — 2012. — Vol. 12, no. 3. — P. 613–661. — DOI: 10.4208/cicp.301110.040811a.
5. Xu Z., Meakin P., Tartakovsky A. M. Diffuse-interface model for smoothed particle hydrodynamics // Physical Review E. — 2009. — Mar. — Vol. 79, no. 3. — DOI:10.1103/physreve.79.036702. — URL: http://dx.doi.org/10.1103/PhysRevE.79.036702.
6. Ambati M., Gerasimov T., De Lorenzis L. A review on phase-field models of brittle fracture and a new fast hybrid formulation // Computational Mechanics. — 2014. — Dec. — Vol. 55. — DOI: 10.1007/s00466-014-1109-y.
7. Provatas N., Elder K. Phase-Field Methods in Materials Science and Engineering. — 10/2010. — DOI: 10.1002/9783527631520.
8. Phase-Field Simulation of Solidification / W. Boettinger [et al.] // Annual Review of Materials Research. — 2002. — Aug. — Vol. 32. — P. 163–194. — DOI: 10.1146/annurev.matsci.32.101901.155803.
9. Simulations of Phase-field Models for Crystal Growth and Phase Separation / A. Cartalade [et al.] // Procedia Materials Science. — 2014. — Dec. — Vol. 7. — P. 72–78. — DOI: 10.1016/j.mspro.2014.10.010.
10. Phase-Field Modeling of Polycrystalline Solidification: From Needle Crystals to Spherulites — A Review / L. Gránásy [et al.] // Metallurgical and Materials Transactions A. — 2014. — Apr. — Vol. 45. — P. 1694–1719. — DOI: 10.1007/s11661-013-1988-0.
11. Phase-field-crystal models for condensed matter dynamics on atomic length and diffusive time scales: an overview / H. Emmerich [et al.] // Advances in Physics. — 2012. — July. — Vol. 61. — P. 665–743. — DOI: 10.1080/00018732.2012.737555.22
12. Asadi E., Asle Zaeem M. A Review of Quantitative Phase-Field Crystal Modeling of Solid–Liquid Structures // JOM. — 2014. — Dec. — Vol. 67. — DOI: 10.1007/s11837-014-1232-4.
13. Using the phase-field crystal method in the multi-scale modeling of microstructure evolution / N. Provatas [et al.] // JOM. — 2007. — July. — Vol. 59, no. 7. — P. 83–90. — DOI:

10.1007/s11837-007-0095-3. — URL: https://doi.org/10.1007/s11837-007-0095-3.
14. Zipunova E., Savenkov E. On the Diffuse Interface Models for High Codimension Dispersed Inclusions // Mathematics. — 2021. — Vol. 9, no. 18. — P. 2026. — DOI: https://doi.org/10.3390/math9182206. — URL: https://doi.org/10.3390/math9182206.
15. Zipunova E., Kuleshov A., Savenkov E. Nonisothermal diffuse interface model for electrical breakdown channel propagation // Sib. Zh. Ind. Mat. — Moscow, 2022. — Vol. 25, issue 1. — P. 35–53. — DOI: https://doi.org/10.33048/SIBJIM.2022.25.103. — URL: https://doi.org/10.33048/SIBJIM.2022.25.103.
16. Bakhvalov N. S., Zhidkov N. P., Kobelkov G. N. Numerical methods. — 8th ed. (electronic). — Moscow : BINOM. Labotarory of knowledge, 2015.
17. Kalitkin N. N. Numerical methods. — 2nd ed. — Saint Petersburg : BHV-Petersburg, 2011.